Dynamic optical transfer function: a function to characterize random motion degraded image

Yanqiao Zhao, Jiubin Tan[*], Jian Liu

Center of Ultra-precision Optoelectronic Instrument Engineering, Harbin Institute of Technology, Harbin 150080, China

Received 10 October 2014, www.cmnt.lv

Abstract

Previous DOTF model is only for static, uniform motion and high speed harmonic vibration. In order to characterize random motion-blurred image, an arbitrary motion DOTF model was built, and it is a function of displacement s(t) of the motion image. The displacement function is no limits to any motion type, and we rigorous derived previously known DOTF expressions for static, uniform motion and high speed harmonic vibration, it is therefore concluded that our DOTF model can be developed for random motion. At last, an experiment was developed to verify our DOTF model.

Keywords: motion-blurred image, DOTF, random motion

1 Introduction

Machine vision and computer vision technology are already widely used in the field of industry, agriculture, etc [1]. However, relative motion between the image sensor and the object during imaging will cause the image degradation, what's more, motion degradation is generally much more severe than that from other factors. So, in order to improve the imaging quality, we have to quantitatively characterize the motion-blurred image and restore it. Dynamic optical transfer function (DOTF) is an image quality evaluation function to characterize this motion degradation, and it is also widely used for restoring motion-blurred image.

The research of DOTF can be tracked back to 1960s. Trott derived the DOTF expressions for uniform motion and high frequency harmonic vibration [2]. Based on Trott's work, Hadar proposed DOTF calculating methods in the space domain and in the spatial frequency domain separately [3, 4]. Later, a series of theoretical analysis and experiments were proposed to prove the correctness of the DOTF calculating methods [5-8]. From then on, DOTF were more and more applied to characterize the motion degradation and restore the motion-blurred image.

In the field of image quality evaluation, the uniform motion DOTF model was used to evaluate the display performance of LCD [9-11], and it suggests that the LCD is a low-pass dispaly device. The harmonic vibration DOTF model was used to evaluate the imaging quality of a push-broom CCD camera [12, 13], and it suggests that the image quality will not change no matter what the Vibration frequency is. Jingyu Liao [14] and Hanzhou Guo [15] used the DOTF model to evaluate the image quality of the aerial camera, and the research results shows that

harmonic vibration is more harmful than uniform motion at the same displacement.

In the field of image restoration, an image restoration method was proposed based on harmonic vibration DOTF model [16]. According to the motion of lung is approximated as harmonic vibration, the restoration method in [16] was used to recover motion-blurred lung image [17]. In [18], an analytical approach for estimating the vibration DOTF from the measured system DOTF by the frequency response of the sensor was present. The goal of this research is to build an automatic system for restoring pictures blurred by vibration.

However, because the existing DOTF models are limited to uniform motion and high frequency harmonic vibration, image quality evaluation and image restoration are aim at the motion-blurred image only for these two motion types, and for other motion type, the existing DOTF models can't be applied to characterize and restore the motion-blurred image.

The purpose and the main advantage of this paper are building a DOTF model for random motion. The remainder of this paper is organized as follows: In Section 2, according to the frequency domain definition of DOTF, our random motion DOTF model is built. In order to verify our DOTF model can be applied to random motion, our DOTF is compared with the existing models in Section 3. Section 4 presents experiment results and related discussions. Finally, the paper is concluded in Section 5.

2 The random motion DOTF model

2.1 CONTRAST AND PHASE OF THE INPUT COSINE PATTERN

A motion cosine input pattern can be described as:

---

[*] *Corresponding author's* e-mail: jbtan@hit.edu.cn

$$I = 1 + C \cdot \cos(2\pi f(x - s(t)) + \varphi) , \tag{1}$$

where C, f, x, $s(t)$, and φ represent the amplitude, spatial frequency, position, initial phase, and motion function of the pattern separately. The function $s(t)$ is not restricted by any motion type, so the function in Equation (1) can describe random motion of the pattern.

According to the definition of the contrast, the contrast of the input pattern is:

$$C_I = \frac{I_{\max} - I_{\min}}{I_{\max} + I_{\min}} = \frac{(1+C) - (1-C)}{(1+C) + (1-C)} = C . \tag{2}$$

If the exposure time of the time-delay imaging system is from t_s to $t_s + t_e$, and $s(t_s)=0$, the phase of the pattern at t_s is:

$$\theta_I = 2\pi f x + \varphi . \tag{3}$$

2.2 CONTRAST AND PHASE OF THE INPUT PATTERN

The imaging process is an integral average one for time, so the output image can be calculated as:

$$O = \frac{1}{t_e} \int_{t_s}^{t_s+t_e} I dt . \tag{4}$$

We can get the output pattern function by substituting Equation (1) into the Equation (4):

$$O = 1 + C[\cos(2\pi f x + \varphi) \cdot CI + \sin(2\pi f x + \varphi) \cdot SI] , \tag{5}$$

where:

$$\begin{cases} CI = \dfrac{1}{t_e} \displaystyle\int_{t_s}^{t_s+t_e} \cos(2\pi f s(t)) dt \\[2mm] SI = \dfrac{1}{t_e} \displaystyle\int_{t_s}^{t_s+t_e} \sin(2\pi f s(t)) dt \end{cases} . \tag{6}$$

If:

$$\begin{cases} \cos\phi = \dfrac{CI}{\sqrt{CI^2 + SI^2}} \\[3mm] \sin\phi = \dfrac{SI}{\sqrt{CI^2 + SI^2}} \end{cases} , \tag{7}$$

Equation (5) can be written as:

$$O = 1 + C \cdot \sqrt{CI^2 + SI^2} \cdot \cos(2\pi f x + \varphi - \phi) . \tag{8}$$

Comparing Equation (8) with Equation (1), it can be concluded that the output signal is also a cosine pattern, which has the same spatial frequency as the input one, but different contrast and phase. We can calculate the contrast and the phase of the output pattern, and the results are:

$$\begin{cases} C_O = C \cdot \sqrt{CI^2 + SI^2} \\[2mm] \theta_O = 2\pi f x + \varphi - \phi \end{cases} . \tag{9}$$

2.3 CONTRAST AND PHASE TRANSFER RULES OF THE COSINE IMAGE

The C_0 in Equation (9) is divided by the C_I in Equation (2), DMTF can be calculated. The θ_0 in Equation (9) subtract the θ_I in Equation (3), DPTF can be also obtained. The calculation results are shown in Equation (10):

$$\begin{cases} DMTF = \dfrac{C_O}{C_I} = \sqrt{CI^2 + SI^2} \\[2mm] DPTF = \theta_O - \theta_I = -\phi \end{cases} . \tag{10}$$

Using Equation (10), DOTF can be calculated as follows:

$$\begin{aligned} DOTF &= DMTF \cdot e^{i \cdot DPTF} = \\ DMTF&[\cos(DPTF) + i \cdot \sin(DPTF)] = CI - i \cdot SI. \end{aligned} \tag{11}$$

The expressions of the CI and SI in Equation (6) are substituted into Equation (11), we can get:

$$\begin{aligned} DOTF &= \frac{1}{t_e} \int_{t_s}^{t_s+t_e} \cos(2\pi f s(t)) dt - \\ i\frac{1}{t_e} &\int_{t_s}^{t_s+t_e} \sin(2\pi f s(t)) dt = \frac{1}{t_e} \int_{t_s}^{t_s+t_e} \exp(-i2\pi f s(t)) dt. \end{aligned} \tag{12}$$

The expression in the Equation (12) is the finally result of the DOTF model. It shows that the image degradation is only related to the motion function $s(t)$ of the image, so, if the motion trajectory of the motion-blurred image can be get strictly, degradation rules of the degraded image can be exactly described.

3 Theoretical verification of our DOTF model can be applied to random motion

3.1 COMPARASION BETWEEN OUR DOTF MODEL AND THE STATIC ONE

If the input pattern is static during the exposure time, the motion function is: $s(t)=0$, the equation is put into the Equation (12), DOTF=1 can be easily got, and there are:

$$\begin{cases} DMTF = |DOTF| = 1 \\[2mm] DPTF = \arg(DOTF) = 0 \end{cases} . \tag{13}$$

DMTF=1 suggests that the contrast of the output cosine pattern is the same as the one of the input signal, DPTF=0 suggests that the phase of the output cosine pattern is the same as that of the input signal. These results shows that if the input pattern is static, the output one has no contrast reduction and phase shift. This conclusion has been a

broad consensus, so it can be concluded that our DOTF model can be applied to static.

3.2 COMPARASION BETWEEN OUR DOTF MODEL AND THE UNIFORM MOTION ONE

If the input pattern is in uniform motion type, the motion function is $s(t)=vt$, and we put this function into the Equation (12), the following result can be got:

$$DOTF = \frac{1}{t_e} \int_{t_s}^{t_s+t_e} \exp(-i2\pi f v t)dt = \qquad (14)$$
$$\mathrm{sinc}(\pi f v t_e)\exp[\pi f v (2t_s + t_e)]$$

According to the definition of the DMTF and the DPTF, we can obtain:

$$\begin{cases} DMTF = |DOTF| = |\mathrm{sinc}(\pi f v t_e)| \\ DPTF = \begin{cases} \pi f v(2t_s + t_e), \mathrm{sinc}(\pi f v t_e) > 0 \\ \pi - \pi f v(2t_s + t_e), \mathrm{sinc}(\pi f v t_e) < 0 \end{cases} \end{cases} \qquad (15)$$

The results in the Equation (15) are the same as those in the Ref. [7], so it can be concluded that our DOTF model can be applied to uniform motion.

3.3 COMPARASION BETWEEN OUR DOTF MODEL AND THE HIGH FREQUENCY HARMONIC VIBRATION ONE

If the input pattern to be of the form:

$$s(t) = D\cos(\omega t + \varphi') , \qquad (16)$$

where D is the amplitude, ω represents the spatial frequency, φ' denotes the phase of the vibration function. In order to make Equation (16) equal to the vibration function of the existing DOTF model, we set:

$$\begin{cases} s(t_s) = D\cos(\omega t_s + \varphi') = \pm D \\ t_e = n \cdot \frac{T}{2} = \frac{n}{2} \cdot \frac{2\pi}{\omega} = \frac{n\pi}{\omega}, (n \in Z) \end{cases} \qquad (17)$$

The following equation can be easily obtained.

$$DOTF = \frac{1}{t_e} \int_{t_s}^{t_s+t_e} \exp[-i2\pi f D\cos(\omega t + \varphi')]dt =$$
$$\frac{1}{\omega t_e} \int_{t_s}^{t_s+\frac{n\pi}{\omega}} \exp[-i2\pi f D\cos(\omega t + \varphi')]d(\omega t + \varphi') \qquad (18)$$

The $\omega t+\varphi'$ is marked as θ, the Equation (18) can be written as:

$$DOTF = \frac{1}{n\pi} \int_{\omega t_s+\varphi'}^{\omega t_s+n\pi+\varphi'} \exp(-i2\pi f D\cos\theta)d\theta =$$
$$\begin{cases} \frac{1}{n\pi} \int_0^{n\pi} \exp(-i2\pi f D\cos\theta)d\theta, s(t_s) = D \\ \frac{1}{n\pi} \int_{\pi}^{(n+1)\pi} \exp(-i2\pi f D\cos\theta)d\theta, s(t_s) = -D \end{cases} \qquad (19)$$

The limit of integration in Equation (19) can be expressed as combination of the one from $2k\pi$ to $(2k+1)\pi$ and the one from $(2k-1)\pi$ to $2k\pi$, no matter $s(t_s) = D$ or $s(t_s) = -D$. What's more, it is easily to be proved:

$$\int_{2k\pi}^{(2k+1)\pi} \exp(-i2\pi f D\cos\theta)d\theta =$$
$$\int_{(2k-1)\pi}^{2k\pi} \exp(-i2\pi f D\cos\theta)d\theta = \int_0^{\pi} \exp(-i2\pi f D\cos\theta)d\theta. \qquad (20)$$

So Equation (19) can be written as:

$$DOTF = \frac{1}{\pi} \int_0^{\pi} \exp(-i2\pi f D\cos\theta)d\theta . \qquad (21)$$

The modulation of the DOTF in Equation (21) is:

$$DMTF = \left| \frac{1}{\pi} \int_0^{\pi} [\cos(i2\pi f D\cos\theta) - i\sin(i2\pi f D\cos\theta)]d\theta \right| =$$
$$\left| \frac{1}{\pi} \int_0^{\pi} \cos(i2\pi f D\sin\theta)d\theta \right|. \qquad (22)$$

Equation (22) is the expression of the first kind 0 orders Bessel function at $v=0$ and $z=2\pi f Ds$, so it can be marked as:

$$DMTF = J_0(2\pi f D) . \qquad (23)$$

For DPTF, we can obtain the follow result from the Equation (17):

$$DPTF = [\omega(t_s + t_e) + \varphi'] - [\omega t_s + \varphi']$$
$$= \begin{cases} 0, & n \in odd \\ \pi, & n \in even \end{cases} \qquad (24)$$

The results in Equation (23) and in Equation (24) are the same as those in the [4-7], so it can be concluded that our DOTF model can be applied to high frequency harmonic vibration.

According to the work above, we have proved that our DOTF model can be applied to static, uniform motion and high frequency harmonic vibration, beyond that, the displacement function $s(t)$ is no limit to any motion type, so, our DOTF model can be applied to random motion can be deduced.

4 Experimental verification of our DOTF model

4.1 THE EXPERIMENTAL PRINCIPLE

It takes two aspects to verify the DOTF model. The first one, the DOTF model can be verified by the consistency between the measuring DOTF curve and the theoretical one in the same parameter. The second one, The DOTF curve will change with a parameter changing, so, the DOTF model can be verified by comparing the changing law we get by experiment to the theoretical analysis one.

According to the conclusion in the first section, the DOTF is a function of the motion function $s(t)$, and the $s(t)$ is a integral function of the velocity, so the DOTF is also a function of the velocity, and it can be written as:

$$DOTF = \frac{1}{t_e}\int_{t_0}^{t_n}\exp(-i2\pi f\int_0^t v(\tau)d\tau)dt . \quad (25)$$

If the velocity changes from v into kv, the DOTF in Equation (25) changes into:

$$DOTF = \frac{1}{t_e}\int_{t_0}^{t_n}\exp(-i2\pi f\int_0^t kv(\tau)d\tau)dt =$$

$$\frac{1}{t_e}\int_{t_0}^{t_n}\exp(-i2\pi(kf)\int_0^t v(\tau)d\tau)dt. \quad (26)$$

Form Equation (26), we can see the coefficient k shifts form the velocity to the spatial frequency, and it shows that the DOTF curve will expand and contract in the spatial frequency direction with the change of velocity.

4.2 THE EXPERIMENTAL DEVICE

Based on the experimental thinking above, an experimental device is built (Figure 1).
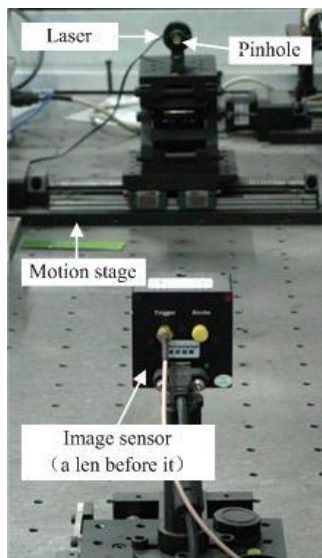
FIGURE 1 Experimental device

In the object space, there is a 20mW laser, and in front of the laser, there is a 5μm diameter pinhole. The laser and the pinhole combine into a point light source, and it is set on a motion stage controlled by a stepper motor controller. In the image space, there is an image sensor whose pixel distance is 5.2μm, and the distance between the pinhole to the image sensor is 1000mm. between the point light source and the image sensor, there is a 50mm lens. The light emitted from the point light source, focused to the image sensor by the lens.

In the geometrical optics theory, focal length, object distance, and image distance satisfy the following relationships:

$$\begin{cases} l'-l = 1000\,\text{mm} \\ f' = -f = 50\,\text{mm} \\ f'/l'+f/l = 1 \end{cases} \quad (27)$$

where $-l$ and l' represent the object distance and the image distance separately, $-f$ and f' denote the object space focal length and the image space focal length separately.

According to the object image distance equation, we got l'=52.7864mm, l=–947.2136mm, and we can calculated the lateral magnification of the imaging system is –0.0557.

4.3 THE EXPERIMENTAL RESULTS

In the experiment, the exposure time of the image sensor was set to 1s, and the speeds of the point light source were set to 2442.5μm/s, 4882.5μm/s, and 9767.5μm/s. According to the lateral magnification of the imaging system is -0.0557, the displacement of the point image on the surface of the image sensor are 136μm, 272μm, and 544μm. In the above parameters, three motion-blurred images were obtained and shown in Figures 2 a-c.
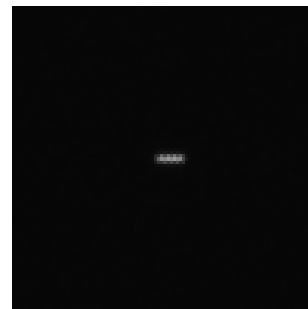
a)
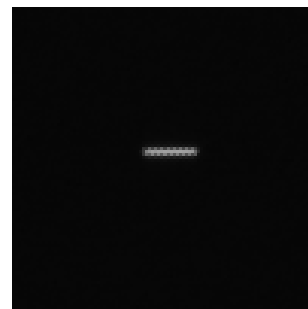
b)
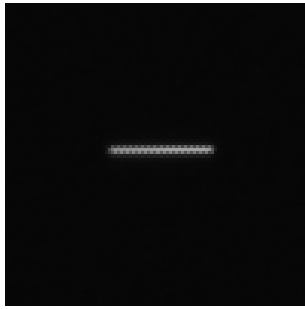
c)

FIGURE 2 Motion-blurred images at different displacements:
a) 136μm, b) 272μm, c) 544μm

The Fourier transform of Figures 2 a-c are three experimental DMTF-spatial frequency arrays. According to the resolution of the motion-blurred image is 100×100, and the pixel length is 5.2μm, we can obtain the spatial frequency of the motion-blurred image is an arithmetic progression with initial term of 0 and common difference of 1.92lp/mm. The experimental DMTF-spatial frequency arrays are shown in Tables 1-3.

TABLE 1 The experimental DMTF-spatial frequency arrays at 136μm displacement

Spatial frequency (lp/mm)	DMTF
0.00	1.00
1.92	0.98
3.85	0.94
5.77	0.86
7.69	0.77
9.62	0.66
11.54	0.55
13.46	0.44
15.38	0.34
17.31	0.24
19.23	0.15
21.15	0.07
23.08	0.02
25.00	0.06

TABLE 2 The experimental DMTF-spatial frequency arrays at 272μm displacement

Spatial frequency (lp/mm)	DMTF
0.00	1.00
1.92	0.95
3.85	0.81
5.77	0.61
7.69	0.37
9.62	0.15
11.54	0.02
13.46	0.13
15.38	0.18
17.31	0.16
19.23	0.11
21.15	0.04
23.08	0.02
25.00	0.06

TABLE 3 The experimental DMTF-spatial frequency arrays at 544μm displacement

Spatial frequency (lp/mm)	DMTF
0.00	1.00
1.92	0.82
3.85	0.40
5.77	0.03
7.69	0.20
9.62	0.14
11.54	0.02
13.46	0.12
15.38	0.08
17.31	0.02
19.23	0.08
21.15	0.05
23.08	0.02
25.00	0.05

The three displacement parameters and the spatial frequency arithmetic progression were put into the DMTF function in the Equation (13), the theoretical DMTF-spatial frequency arrays were obtained and shown in Tables 4-6.

TABLE 4 The theoretical DMTF-spatial frequency arrays at 136μm displacement

Spatial frequency(lp/mm)	DMTF
0.00	1.00
1.92	0.99
3.85	0.96
5.77	0.90
7.69	0.83
9.62	0.74
11.54	0.64
13.46	0.53
15.38	0.41
17.31	0.30
19.23	0.19
21.15	0.09
23.08	0.00
25.00	0.08

TABLE 5 The theoretical DMTF-spatial frequency arrays at 272μm displacement

Spatial frequency(lp/mm)	DMTF
0.00	1.00
1.92	0.96
3.85	0.83
5.77	0.64
7.69	0.41
9.62	0.19
11.54	0.00
13.46	0.14
15.38	0.21
17.31	0.21
19.23	0.17
21.15	0.09
23.08	0.00
25.00	0.07

TABLE 6 The theoretical DMTF-spatial frequency arrays at 544μm displacement

Spatial frequency (lp/mm)	DMTF
0.00	1.00
1.92	0.83
3.85	0.41
5.77	0.00
7.69	0.21
9.62	0.17
11.54	0.00
13.46	0.12
15.38	0.10
17.31	0.00
19.23	0.08
21.15	0.08
23.08	0.00
25.00	0.06

In order to comparing the experimental result with the theoretical one, the experimental DMTF-spatial frequency arrays and the theoretical ones were draw together in the form of curves and shown in Figure 3.
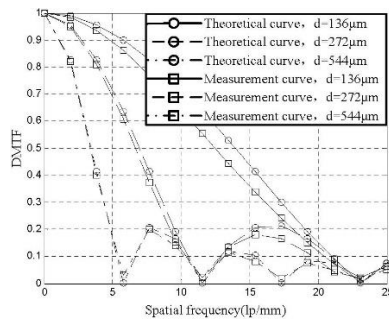
FIGURE 3 Comparison between the theoretical DMTF curves and the experimental DMTF ones

The theoretical curves was compared with the experimental ones in the same displacement, we can see that no matter what the displacement is, they have a good consistency. On that basis, the varying law of the DOTF model with the velocity is the same as the experimental one. So, Based on the experiment and the analysis above, the correctness of our DOTF model was proved.

References

[1] Wang X, Dong X 2013 Hand gesture tracking and recognition technology based on computer vision *Computer Modelling and New Technologies* **17**(4) 191-5
[2] Trott T 1960 The Effects of Motion on Resolution *Photogrammetric Engineering* **26**(5) 819-27
[3] Hadar O, Fisher M, Kopeika N S 1991 Numerical calculation of Image motion and vibration modulation transfer function *Proceedings of the SPIE* **1482** 79-91
[4] Hadar O, Dror I, Kopeika N S 1991 Numerical calculation of image motion and vibration modulation transfer functions: a new method *Proceedings of the SPIE* **1533** 61-74
[5] Wulich D, Kopeika N S 1987 Image resolution limits resulting from mechanical vibrations *Optical engineering* **26**(6) 266529
[6] Rudoler S, Hadar O, Fisher M, Kopeika N S 1991 Image Resolution Limits Resulting from Mechanical Vibrations Part II: Experiment *Optical Engineering* **30**(5) 577-89
[7] Hadar O, Fisher M, Kopeika N S 1992 Image resolution limits resulting from mechanical vibrations Part III: numerical calculation of modulation transfer function *Optical engineering* **31**(3) 581-9
[8] Hadar O, Dror I, Kopeika N S 1994 Image resolution limits resulting from mechanical vibrations Part IV: real-time numerical calculation of optical transfer functions and experimental verification[J]. Optical engineering **33**(2) 566-78
[9] Zhao C, Li X 2007 Study of LCDs Motion Blur Based on Modulation Transfer Function (MTF) *Chinese Journal Of Electron Devices* **30**(1) 225-27 *(in Chinese)*

[10] Zhang Y, Teunissen K, Song W, Li X 2008 Dynamic Modulation Transfer Function: A Method to Characterize the Temporal Performance of Liquid-crystal Displays *Optics Letters* **33**(6) 533-5.
[11] Zhao D, Zhang Y, Li X 2009 Measurement and Calculation of LCDs' Dynamic Modulation Transfer Function *Chinese Journal Of Electron Devices* **32**(1) 1-3 *(in Chinese)*
[12] Xu P, Hao Q, Huang C, Wang Y 2002 Degradation of image quality caused by vibration in push-broom camera *Proceedings of SPIE* **4927** 813-7
[13] Xu P, Hao Q, Huang C, Wang Y 2003 Degradation of modulation transfer function in push-broom camera caused by mechanical vibration *Optics & Laser Technology* **35**(7) 547-52
[14] Liao J, Gao X, Liang W 2011 Dynamic MTF Analysis and Research for Aerial Camera *Acta Photonica Sinica* **40**(5) 679-83
[15] Guo H, Lu H, Qu L 2013 Relation of line transfer period error and dynamic MTF of TDICCD in remote sensing camera *Optics and Precision Engineering* **21**(8) 2195–2200
[16] Yitzhaky Y, Boshusha G, Levy Y, Kopeika N S 2000 Restoration of an image degraded by vibrations using only a single frame *Optical engineering* **39**(8) 2083-91
[17] Arbel D, Hadar O, Kopeika N S 2001 Medical image restoration of dynamic lungs using optical transfer function of lung motion *Journal of Biomedical Optics* **6**(2) 193-9
[18] Raiter S, Hadar O, Kopeika N S 2002 Influence of motion sensor error on image restoration from vibrations and motion *Optical Engineering* **41**(12) 3276-82

5 Conclusions

In this paper we have built a DOTF model, and it is a function of displacement $s(t)$ of the motion image. Using our DOTF model, we rigorous derived previously known DOTF expressions for static, uniform motion and high frequency harmonic vibration, according to the displacement function $s(t)$ of the motion image is no limits to any motion type, it is therefore concluded that our DOTF model can be developed for random motion. An experiment was developed to verify this conclusion. Our DOTF model can be implemented in image motion degradation analysis and in restoration of arbitrary motion degraded image.

Acknowledgments

Authors	
	Yanqiao Zhao , September 1983, Harbin, Heilongjiang Province, P.R. China. **Current position, grades**: PhD. **University studies**: Center of Ultra-precision Optoelectronic Instrument Engineering, Harbin Institute of Technology, Harbin 150080, China. **Scientific interests**: theory and practical technology of DOTF.
	Jiubin Tan, March 1955, Harbin, Heilongjiang Province, P.R. China. **Current position, grades**: PhD, professor. **Scientific interests**: ultra precision measurement technology and instruments, ultra precision laser measuring and detecting technology.
	Jian Liu, August 1974, Harbin, Heilongjiang Province, P.R. China. **Current position, grades**: PhD, professor **Scientific interests**: diffraction optics and photoelectric measuring and testing.